Decadal variations in the global atmospheric land temperatures

Richard A. Muller,[1,2,3] Judith Curry,[4] Donald Groom,[2] Robert Jacobsen,[1,2] Saul Perlmutter,[1,2] Robert Rohde,[3] Arthur Rosenfeld,[1,2] Charlotte Wickham,[5] and Jonathan Wurtele[1,2]

Received 22 April 2013; revised 28 April 2013; accepted 30 April 2013; published 10 June 2013.

[1] Interannual to decadal variations in Earth global temperature estimates have often been identified with El Niño Southern Oscillation (ENSO) events. However, we show that variability on time scales of 2–15 years in mean annual global land surface temperature anomalies T_{avg} are more closely correlated with variability in sea surface temperatures in the North Atlantic. In particular, the cross-correlation of annually averaged values of T_{avg} with annual values of the Atlantic Multidecadal Oscillation (AMO) index is much stronger than that of T_{avg} with ENSO. The pattern of fluctuations in T_{avg} from 1950 to 2010 reflects true climate variability and is not an artifact of station sampling. A world map of temperature correlations shows that the association with AMO is broadly distributed and unidirectional. The effect of El Niño on temperature is locally stronger, but can be of either sign, leading to less impact on the global average. We identify one strong narrow spectral peak in the AMO at period 9.1 ± 0.4 years and p value of 1.7% (confidence level, 98.3%). Variations in the flow of the Atlantic meridional overturning circulation may be responsible for some of the 2–15 year variability observed in global land temperatures.

Citation: Muller, R. A., J. Curry, D. Groom, R. Jacobsen, S. Perlmutter, R. Rohde, A. Rosenfeld, C. Wickham, and J. Wurtele (2013), Decadal variations in the global atmospheric land temperatures, *J. Geophys. Res. Atmos.*, *118*, 5280–5286, doi:10.1002/jgrd.50458.

1. Introduction

[2] The average earth land surface temperature, T_{avg}, is a key indicator of climate change. Detailed analyses of T_{avg} have been reported by three major teams: the National Oceanic and Atmospheric Administration (NOAA) [*Menne and Williams*, 2005] (the NOAA average land temperature estimate can be downloaded at ftp.ncdc.noaa.gov/pub/data/anomalies/monthly.land.90S.90N.df_1901-2000mean.dat), the NASA Goddard Institute for Space Studies (GISS) [*Hansen et al*., 2010] (updated land temperature data available at data.giss.nasa.gov/gistemp/graphs/), and a collaboration of the Hadley Centre of the UK Meteorological Office with the Climate Research Unit of East Anglia (HadCRU) [*Jones and Moberg*, 2003; *Brohan et al*., 2005]. (Temperature data are available at http://hadobs.metoffice.com/hadcrut3/diagnostics/comparison.html.) Results from their analysis are shown in Figure 1. The time period in the plot begins at 1950 since a large number of new stations were introduced at that time; the uncertainties prior to 1950 are substantially larger. Note that in this paper, we focus on the land-only temperature average—not including oceans—so that the time series will not directly include the ocean data that we will use for our correlation analysis.

[3] Also shown in Figure 1 is a new estimate of the Earth atmospheric land surface temperature that we created from data independent of those used by the other three groups. We obtained this estimate by choosing 2000 sites randomly from a list of approximately 30,964 temperature recording stations worldwide that had not been used by NOAA, GISS, or HadCRU. Each temperature record was adjusted by an additive parameter, one per record, to bring it into a best least squares fit with the other records; details of this procedure are described by *Rohde et al*. [2013a]. The statistical techniques used (Kriging) are designed to compensate for sampling biases in station coverage. This permits a random selection of stations to be made without giving excessive weight to heavily sampled regions, such as North America and Europe. No adjustments or corrections were made for systematic effects such as urban heat island warming or change of instrumentation. Despite these limitations, the virtue of this estimate is that it is derived from data independent from those previously used. Because of this, the qualitative agreement with the prior estimates confirms that the fluctuations are true indicators of climate and not artifacts of data selection and processing. The four curves show a broad trend of "global warming" with some unevenness; the lack of warming from 1950 to 1975 has been attributed to a combination of natural and anthropogenic factors, especially the cooling effect of increased aerosol pollution [*Jones and Moberg*, 2003].

[1]Department of Physics, University of California, Berkeley, California, USA.
[2]Lawrence Berkeley National Laboratory, Berkeley, California, USA.
[3]Berkeley Earth, Berkeley, California, USA.
[4]Georgia Institute of Technology, Atlanta, Georgia, USA.
[5]Department of Statistics, Oregon State University, Corvallis, Oregon, USA.

Corresponding author: R. A. Muller, The Berkeley Earth Program, 2831 Garber St., Berkeley, CA 94705, USA. (ramuller@lbl.gov)

2169-897X/13/10.1002/jgrd.50458

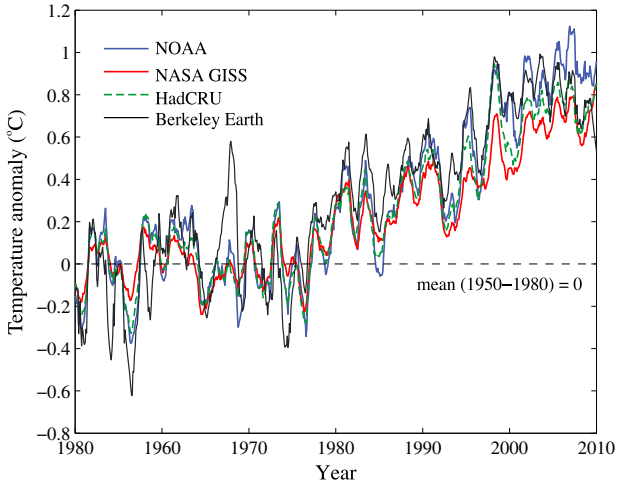

Figure 1. Global land temperature estimates T_{avg}, smoothed by a 12 month moving average. The temperature anomaly is the difference between the estimated temperature and the mean in the period 1950–1980 for each temperature series. Note the similarity of many of the short-term fluctuations with periods 2–15 years. The Berkeley Earth data were randomly chosen from 30,964 sites that were not used by the other groups.

2. Decadal (2–15 Year) Variations

[4] Much attention has been given to the small T_{avg} maxima of 1998 and 2005. The maximum in 1998 occurred during a very strong El Niño and is plausibly associated with that oceanic event [*Trenberth et al.*, 2002]. In this study, we examined the annually averaged global land temperature time series to study their possible correlation not only with the El Niño Southern Oscillation (ENSO) index (we used the Nino 3.4 data available from the Earth System Research Laboratory, Physical Sciences Division (www.esrl.noaa.gov/psd/data/correlation/nina34.data) and from the NOAA Climate Prediction Center (www.cpc.ncep.noaa.gov/data/indices/wksst.for)) but also with the Atlantic Multidecadal Oscillation (AMO) [*Schlesinger and Ramankutty*, 1994; *Enfield et al.*, 2001], the Pacific Decadal Oscillation (PDO) [*Zhang et al.*, 2007], the North Atlantic Oscillation (NAO) [*Jones et al.*, 1997; *Hurrell*, 1995] (the NAO index data are available from NCAR at www.cgd.ucar.edu/cas/catalog/climind/), and the Arctic Oscillation (AO) [*Thompson and Wallace*, 1998]. Three of these indices—ENSO, AMO, and PDO—are derived from sea surface temperature records: in the equatorial Pacific, the North Atlantic, and the North Pacific, respectively. Two of these, the NAO and the AO, are derived from surface pressure differences at locations in the northern Atlantic and Arctic. We find that the strongest cross-correlation of the decadal fluctuations in land surface temperature is not with ENSO but with the AMO. The AMO index is plotted in Figure 2.

[5] Our analysis used the monthly land surface average temperature records made available by the four groups previously referenced: NOAA, NASA GISS, HadCRU, and ours, the Berkeley Earth Surface Temperature group. The land temperature data were smoothed with a 12 month running average (boxcar smoothing); this removes high-frequency (e.g., monthly) changes. The data prior to 1950 were noisier than the subsequent data, primarily because the number of stations was smaller, and for that reason, we restricted the period for our analysis to 1950–2010.

[6] To emphasize the decadal-scale variations, the long-term changes in the temperature records and oceanic indices were "prewhitened." This is a process to remove a large signal that is not being studied in order to reduce bias in the remainder. To do this, we fit each record (yearly data sets) separately to a fifth-order polynomial in time using a linear least squares regression; we subtracted the respective fits and normalized the results to unit mean square deviation. This procedure effectively removes slow changes such as global warming and the ~70 year cycle of the AMO, and gives each record zero mean. The 12 month smoothing removes high-frequency (e.g., monthly) changes. All of the remaining analysis in this paper is based on the prewhitened temperature records and oceanic indices.

[7] The four temperature estimates after this conditioning are shown in Figure 3a. In Figures 3b and 3c, these four temperature estimates were averaged and compared, in turn, to the conditioned AMO and ENSO. In Figure 3d, we directly compare the AMO and ENSO decadal variations.

3. Difference and Correlation Analysis

[8] Visual inspection of Figure 3 suggests that the AMO fluctuations match the temperature variations better than does the ENSO index almost everywhere, perhaps the only prominent exception being 1968–1973. This impression is verified by calculating the RMS (root-mean-square) differences of pairs of plots. The results are shown in Table 1. Note that the RMS of the difference between ENSO and T_{avg} is over 50% larger than that of the difference between AMO and T_{avg}. The RMS of the difference between AMO and ENSO is 67% larger than that of AMO and T_{avg}. The "random" signal, which is put to show the RMS expected when there is no correlation, was created by breaking the ENSO signal into 10 parts and randomly scrambling them; the RMS of the difference between it and the AMO agrees with the theoretical expectation of $\sqrt{2}$.

[9] To quantify further the relationship between T_{avg} and AMO and ENSO, we performed a correlation analysis. Correlation $C(A, B)$ is a measure of the linear time invariant dependence between two time series $\{A(t)\}$ and $\{B(t)\}$.

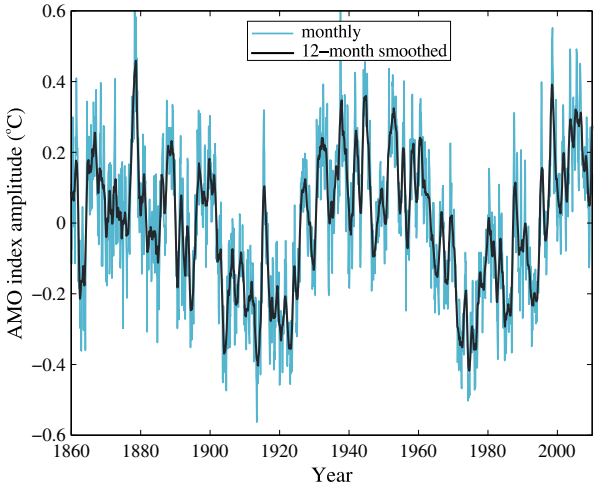

Figure 2. The AMO index. The pattern is dominated by the 65–70 year multidecadal oscillation that gave the index its name. In this paper, we are more interested in the short-term 2–15 year variations that are evident in the 12 month smoothed curve.

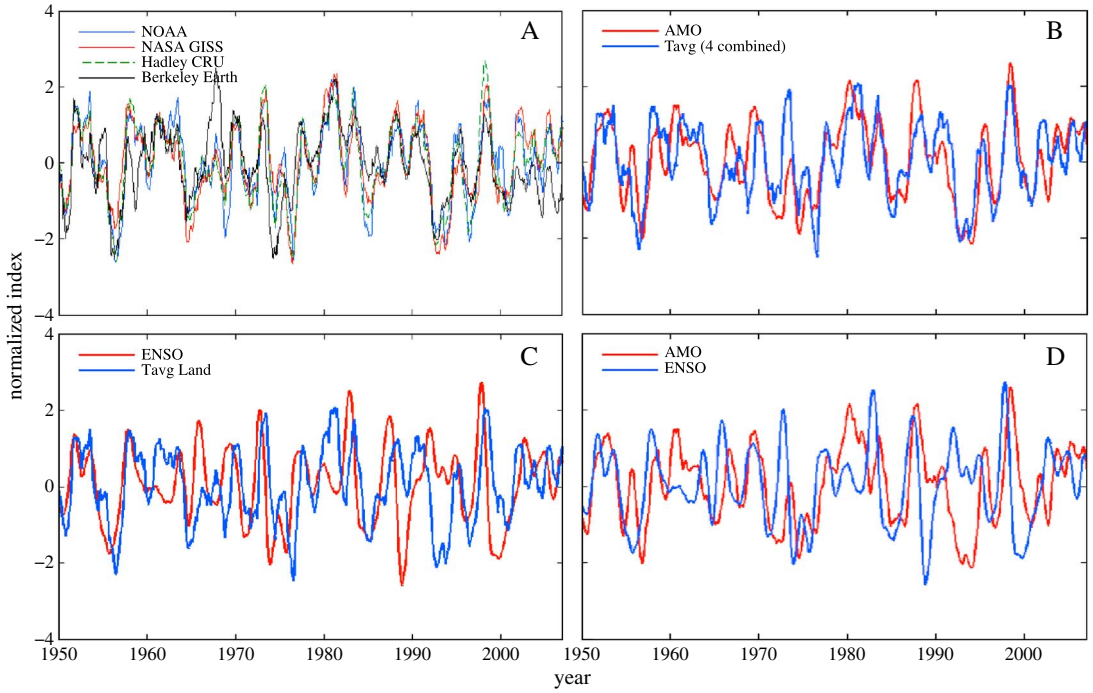

Figure 3. Decadal fluctuations in surface land temperature estimates and in oceanic indices. The long-term variability was suppressed by removing the least squares fit fifth-order polynomial from each curve. (a) Four detrended estimates of the Earth land surface temperature. Agreement is strong, even though the Berkeley Earth estimate used a non-overlapping data set. (b) The four temperature records were averaged and are shown in blue. The detrended AMO is shown in red. (c) Averaged temperature records compared to ENSO. (d) Detrended AMO compared to detrended ENSO. Note that the AMO agreement in Figure 3b is qualitatively stronger than the ENSO agreement in Figure 3c.

Here A and B represent either prewhitened temperature signals or oceanic indices, normalized to zero mean and unit standard deviation. If we include the possibility of a time delay or lag L between the two signals, then we can define the cross-correlation C as follows:

$$C(A,B;L) = \frac{1}{N(L)}\sum A(t)B(t+L)$$

where A and B have zero mean and unit standard deviation and $N(L)$ is the number of terms in the sum. With this definition, the correlation of a function can vary between -1 and $+1$. At zero lag, the autocorrelation = 1. The value of the correlation at zero lag is commonly called Pearson's correlation coefficient, often designated by r.

[10] The correlation estimates between major temperature records and oceanic indices are shown in Figure 4. In these plots, a peak at 0 lag indicates a direct linear correlation between the data sets. A peak offset from zero also indicates correlation but with one lagging the other by the offset.

[11] The strongest correlation is observed between the estimates of the average land temperature T_{avg} and AMO, the Atlantic Multidecadal Oscillation, with a correlation coefficient $r = 0.65 \pm 0.04$. (In this paper, $\pm$ refers to 1 standard error, frequently called by physicists "one standard deviation.") This is the highest peak in any of the cross-correlation plots we calculated, and it occurs at zero lag. The correlation coefficient for the temperature data with ENSO is substantially less, with $r = 0.49 \pm 0.04$. The error uncertainties were estimated from the variance of the four correlations.

[12] For reference, the maximum correlation between AMO and ENSO in these data is 0.50 ± 0.04, with AMO lagging ENSO by 0.70 ± 0.25 years. This is a somewhat larger lag than the previously reported 3 months in a more detailed analysis of ENSO by *Trenberth et al.* [2002].

[13] To estimate the statistical significance of the AMO r factor, we did a permutation test based on a Monte-Carlo simulation. The AMO prewhitened record contains 16 points at which the index rises through zero; we chopped the record at these points, creating 17 AMO segments. The order of these segments was then permuted randomly and reassembled, creating a simulated AMO. Because of the manner of cutting, the scrambled AMO has many of the same

Table 1. Root-Mean-Square Difference of the Data Shown in Figure 3[a]

Records	RMS
(4 estimates) – T_{avg}	0.26
AMO – T_{avg}	0.75
ENSO – T_{avg}	1.14
AMO – ENSO	1.25
AMO – random	1.41

[a]The first row shows the RMS deviation of the four temperature estimates from T_{avg}, the average of the four. The other entries show the RMS deviation of the signal differences. The "random" signal was generated by breaking ENSO into 10 parts and randomly scrambling them in time.

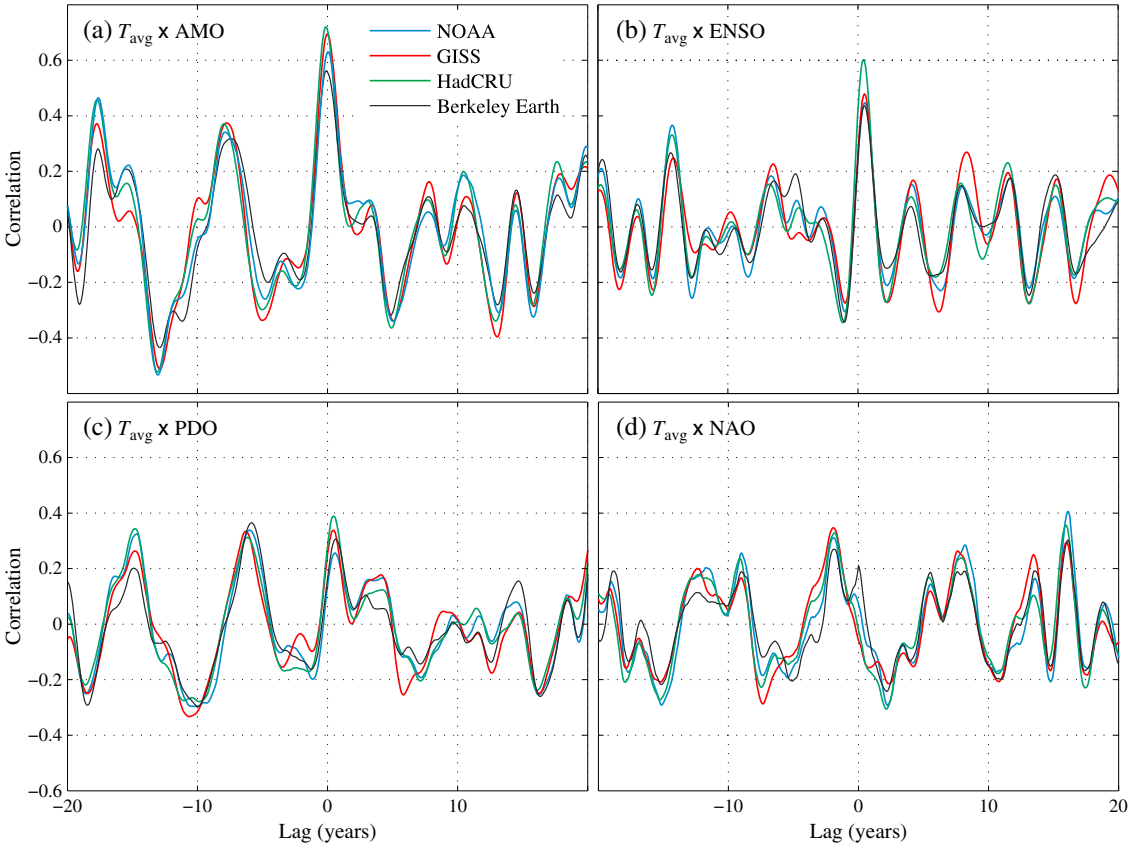

Figure 4. Decadal correlations of the Berkeley Earth land temperature estimates T_{avg} with the (a) AMO index, (b) ENSO index, (c) PDO index, and (d) NAO index. The strongest correlation observed, 0.65 ± 0.04, is with the AMO.

statistical properties as the original AMO; it has the identical amplitude distribution as well as the same number and shapes of peaks and valleys. Indeed, it looks to the eye very much like the original AMO. We generated 1,000,000 of these simulated AMOs and calculated the correlation coefficient r for each of these with the T_{avg} of the Berkeley Earth surface land temperature record. In those 1,000,000 simulated AMO trials, the highest value of r obtained was 0.49, substantially less than the value of 0.65 ± 0.04 obtained with the real AMO, giving a p factor less than 10^{-6}. Of course, it is not too surprising that land temperature estimates are correlated with sea temperature indices; the key observation is that for interannual to decadal variations, it is the AMO that has the strongest correlation, not ENSO or one of the other indices. Based on the same method, we found that none of the peaks in Figures 4c and 4d are statistically significant at the 95% confidence level.

[14] Figure 5a shows the conditioned AMO and PDO indices as a function of time. It can be seen on this plot that PDO generally leads AMO. The correlation is shown in Figure 5b. Although the correlation peaks near zero lag, the bulk of the central correlation peak is at a lag of about 2 years. The periodicity of the correlation plot is an indication of a periodicity in both AMO and PDO that we will discuss next.

[15] It is not possible from the correlations to ascribe causality with any certainty. For example, *Zhang and Delworth* [2007] suggested that the observed AMO leads the inverted PDO index by about 12 years, and discussed the possible mechanism for such an Atlantic-Pacific linkage. On our plot (Figure 5b), this corresponds to the large downward variation at lag of negative 12 years. Such ambiguities could be addressed by mapping the correlation over the world as a function of time.

4. Correlation Map

[16] In Figure 6, we show a map of the decadal correlations of both AMO and ENSO with the NOAA global temperature anomaly map; this map includes oceans as well as land. The association with AMO is broadly distributed and unidirectional. The effect of El Niño on temperature is locally stronger, but can be of either sign, leading to less impact on the global average. The strong correlation of AMO with the Atlantic is, of course, a result of the fact that the AMO is derived from Atlantic temperatures, similarly for the strong correlation between ENSO and the equatorial Pacific. ENSO also shows a strong correlation with the Indian Ocean. On the land, the AMO affects Africa, southern Asia, and Canada; ENSO correlates most strongly to the continents in the Southern Hemisphere. Note its weak correlation to the Atlantic.

[17] Remarkably, neither AMO nor ENSO shows a strong correlation with the temperature in the United States, although ENSO reaches strongly up the west coast of the United States. The variations in the Caribbean, related to the hurricane intensity hitting the southern coast of the

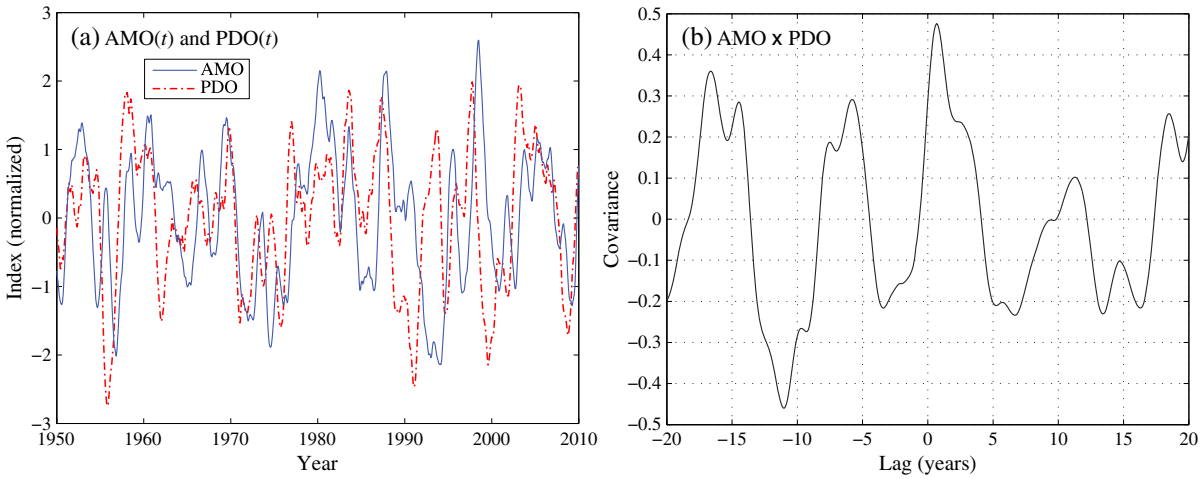

Figure 5. (a) Prewhitened AMO and PDO indices plotted together versus time. It can be seen that PDO leads AMO by about 2.5 years. (b) Correlation of AMO and PDO versus lag. The periodicity of the correlation (4.5 cycles in 40 years of lag) is a result of the apparent presence of a 9 year cycle in both.

United States, are more strongly affected by AMO than by ENSO. The correlation patterns help to explain the larger association observed between AMO and T_{avg} than between ENSO and T_{avg}. ENSO is locally a more intense effect, but it is also a more complex one, giving rise to both correlated and anticorrelated behavior. By contrast, the AMO map shows positive (or neutral) correlation nearly everywhere. Given this, it is not surprising that the simpler AMO association corresponds to a clearer imprint on the large-scale average, T_{avg}.

5. Spectral Analysis

[18] In Figure 7, we show the spectral power for the AMO and PDO prewhitened indices. This spectral power estimate is a periodogram, calculated using a Fourier transform with no taper, padded with zeros to yield intermediate frequencies; the spectral method is described in *Muller and MacDonald* [2000].

[19] In the AMO spectrum, a strong peak appears at a frequency of 0.11 ± 0.005/year and period of 9.1 ± 0.4 years. We place no error bars on this plot because the expected distribution for a power spectrum is exponential, not Gaussian. Instead, we estimate the statistical significance of this peak using the Monte-Carlo approach described earlier. Ten thousand time-scrambled AMO data were used as estimates of random background. In these runs, we obtained a peak (at any frequency) of spectral power level of 18 or greater a total of 170 times. Based on this, we conclude that the probability that the observed peak in the unscrambled data could be due to chance is 170/10,000, i.e., the p value is 1.7%. For the frequency uncertainty, a cycle of fixed frequency 0.1 cycle/year and power amplitude of 18 (same as the observed peak) was injected into a set of 10,000 scrambled AMO sets, and the observed root-mean-square of the frequency distribution was taken to be the frequency uncertainty.

[20] Although the 9.1 year peak in the AMO has high statistical significance, it contains only 30% of the spectral

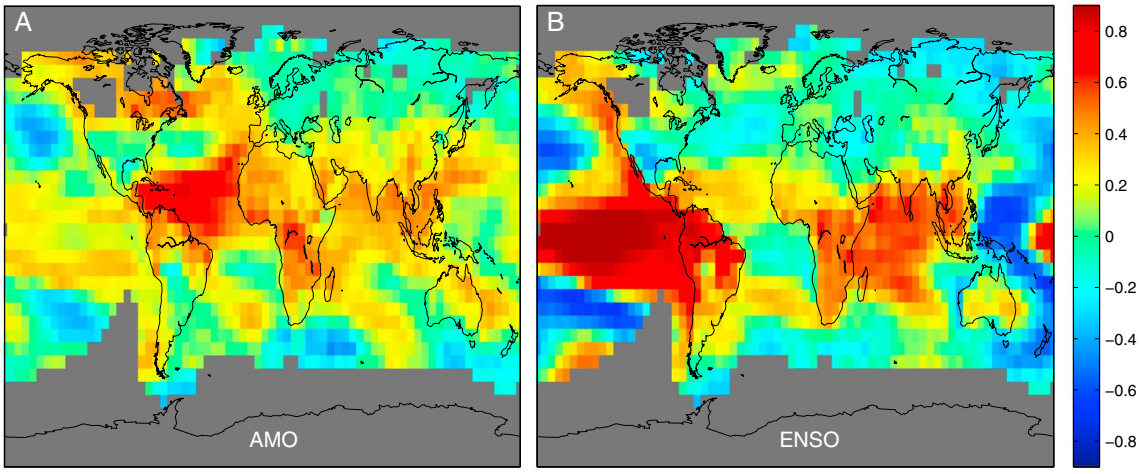

Figure 6. Short-term correlation maps of the filtered (a) AMO and (b) ENSO time series 1950–2010 with similarly filtered temperature time series taken from the Earth's surface temperature map constructed by the NOAA group. Colors show the degree of correlation at each location. AMO is observed to have positive or neutral correlation almost everywhere, while ENSO shows both strong positive and negative correlations.

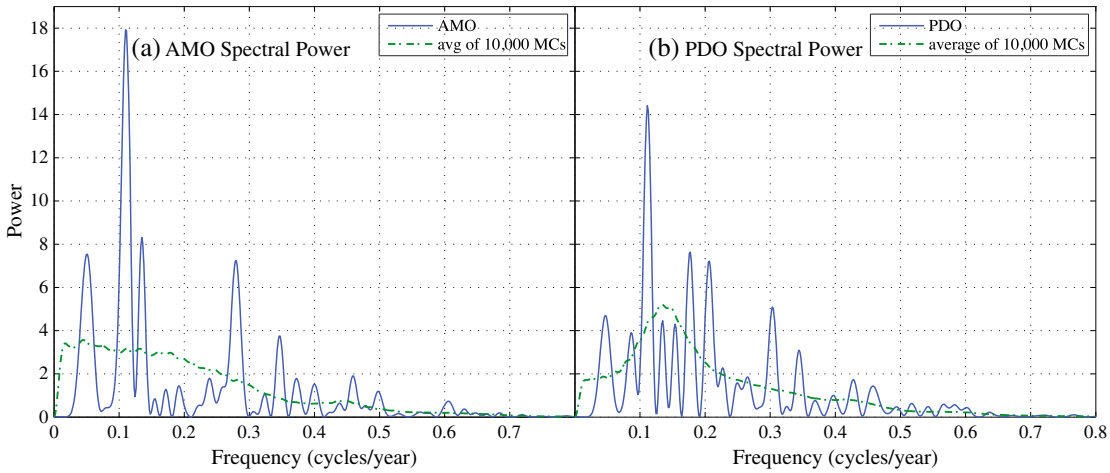

Figure 7. Spectral power in the (a) Atlantic Multidecadal Oscillation and (b) Pacific Decadal Oscillation. The low-frequency oscillations (<0.06/year) have been suppressed by the subtraction of a best fit fifth-order polynomial from each time series prior to calculation of the spectrum; similarly, a 12 month running average eliminated high-frequency (e.g., monthly) fluctuations. A strong peak is observed in the AMO at 0.110 ± 0.005 cycles/year, corresponding to a period of 9.1 ± 0.4 years, at the 98.3% confidence level. The maximum peak in the PDO occurs at a similar frequency, 0.111 ± 0.006, although with a confidence level of 94%.

power; for this reason, its presence is not evident to the eye in Figure 3 or 4.

[21] The highest peak in the PDO spectrum (Figure 7b) has a period of 9.0 ± 0.5 years with amplitude of 14.4 and p value of 6%. None of the other peaks in Figure 6 are statistically significant. We also looked at the spectra of ENSO, NAO, and T_{avg}; we did not find any statistically significant narrow spectral signals, although there is, of course, broad power in the decadal bands.

6. Summary and Discussion

[22] The similarity between the decadal fluctuations in land surface temperature records that use different sources indicates that the fluctuations are physical and not the effect of statistical fluctuations. The 2–15 year variations in AMO, based on sea surface temperature records, strongly correlate with the land record T_{avg}. Although short-term excursions, such as the temperature maximum in 1998, were widely associated with a strong El Niño event, the AMO is more closely associated with variability in the globally average land surface temperature than is ENSO.

[23] For a discussion of the variability of the AMO, see *Frankcombe et al*. [2010], who identified important variability in two time scales: 20–30 years and 50–70 years. In this and much of other analyses prior to ours, the key focus was on longer time scales, and so the data were smoothed with a decade-long running average; such a procedure suppresses the interannual to decadal scale variations (2–15 years) that are the subject of the present paper.

[24] In the interannual to decadal region we studied, there is only one statistically significant spectral peak, with period of 9.1 ± 0.4 years, strong in the AMO, weaker in the PDO. It is not present at a statistically significant level in the land T_{avg} or in ENSO or in other ocean indices that we examined. Spectral analysis of global temperatures by others had previously yielded claims of many frequencies, most of which we conclude are not statistically significant when we analyze them using our Monte-Carlo background estimation. For example, *Scafetta* [2010] reported a forest of 11 spectral peaks based on a multitaper analysis; to each of these peaks, he calculated 99% confidence intervals. He reported seven peaks with periods in the range from 5.99 to 14.8 years. One of these is at our period of 9.1 years; he suggests that this cycle could be induced by lunar tidal variations. However, we find that when we use our Monte-Carlo methods to estimate background, none of his claimed peaks are statistically significant except for the 9.1 year peak; we do not find them in the AMO, PDO, or ENSO.

[25] Correlation does not imply causation. The association between Atlantic sea surface temperature fluctuations and land temperature may simply indicate that both sets of temperatures are responding to the same source of natural variability. However, it is also interesting to consider whether oceanic changes in the AMO may be driving short-term fluctuations in land surface temperature. Such fluctuations might originate as instabilities in the AMO region itself, or they might occur as a nonlinear response to changes elsewhere (such as within the ENSO region).

[26] If the fluctuations originate locally, then they might be associated with natural variations in the meridional overturning circulation (MOC) or from salinity anomaly events [*Dickson et al*., 1988; *Belkin*, 2004]. They could be related to a larger instability in the flow of the thermohaline circulation (the oceanic conveyor belt). Computer simulations of the thermohaline circulation by *Jungclaus et al*. [2005] "show pronounced multidecadal fluctuations of the Atlantic overturning circulation and the associated meridional heat transport. The period of the oscillations is about 70–80 years. The low-frequency variability of the meridional overturning circulation (MOC) contributes substantially to sea surface temperature and sea ice fluctuations in the North Atlantic."

[27] A theory for decadal oscillations in the North Pacific was devised by *Munnich et al*. [1998]. It involves an

interaction between wind and the thermohaline circulation. Such models predict a broad spectrum of frequencies and could drive the structure we see in Figure 3a, but we would not expect such a driving force to result in the narrow 9.1 year peak. For more on exited internal modes, see *Frankcombe et al*. [2010] and *Sévellec et al*. [2009, 2010] and the references therein.

[28] Because there is little time lag between the AMO variability and that of the land surface temperatures, it is possible that one is not driving the other, but that they are varying together, perhaps through dynamics that include wind-driven gyres that could link different ocean basins. These speculations might be addressed by a more detailed study of the correlations between the temperature distributions over the globe.

[29] Given that the 2–15 year variations in world temperature are so closely linked to the AMO raises (or reraises) an important ancillary issue: to what extent does the 65–70 year cycle in AMO contribute to the global average temperature change [*Enfield et al.*, 2001; *Zhang et al*., 2007; *Kerr*, 2000]? Since 1975, the AMO has shown a gradual but steady rise from −0.35°C to +0.2°C (see Figure 2), a change of 0.55°C. During this same time, the land-average temperature has increased about 0.8°C. Such changes may be independent responses to a common forcing (e.g., greenhouse gases); however, it is also possible that some of the land warming is a direct response to changes in the AMO region. If the long-term AMO changes have been driven by greenhouse gases, then the AMO region may serve as a positive feedback that amplifies the effect of greenhouse gas forcing over land. On the other hand, some of the long-term change in the AMO could be driven by natural variability, e.g., fluctuations in thermohaline flow. In that case, the human component of global warming may be somewhat overestimated. However, in a recent analysis covering more than 250 years [*Rohde et al*., 2013b], the long-term temperature changes were well correlated to a simple model that only contained information about CO_2 and volcanic events. The strong association between CO_2 and the long-term warming argues against natural variability as a major contributor to the long-term (century-scale) temperature rise; however, the AMO and other factors may have contributed significant variability on shorter (multidecadal) time scales.

[30] In conclusion, our analysis suggests that strong interannual and decadal variations observed in the average land surface temperature records represent a true climate phenomenon, not only during the years when fluctuations on the time scale of 2–15 years had been previously identified with El Niño events. The variations are strongly correlated with the similar decadal fluctuations observed in the Atlantic Multidecadal Oscillation index, and less so with the El Niño Southern Oscillation index. This correlation could indicate that the AMO plays an important intermediary role in the influence of the Pacific ENSO on world climate; alternatively, it might indicate that variability in the thermohaline flow plays a bigger role than had previously been recognized. The models could be tested by studying the temperature correlations in the ocean as a function of location and time. A 9.1 ± 0.4 year cycle is observed in the prewhitened AMO, but it contributes only 30% to the variance. A similar cycle at 9.0 ± 0.5 years is seen in the PDO.

[31] **Acknowledgments.** This work was done as part of the Berkeley Earth project, organized under the auspices of the Novim Group (www.Novim.org). We thank many organizations for their support, including the Lee and Juliet Folger Fund, the Lawrence Berkeley National Laboratory, the William K. Bowes Jr. Foundation, the Fund for Innovative Climate and Energy Research (created by Bill Gates), the Ann and Gordon Getty Foundation, the Charles G. Koch Charitable Foundation, and three private individuals (M.D., N.G., and M.D.). More information on the Berkeley Earth project can be found at www.BerkeleyEarth.org.

References

Belkin, I. M. (2004), Propagation of the "Great Salinity Anomaly" of the 1990s around the northern North Atlantic, *Geophys. Res. Lett.*, *31*, L08306, doi:10.1029/2003GL019334.

Brohan, P., J. J. Kennedy, I. Harris, S. F. B. Tett, and P. D. Jones (2005), Uncertainty estimates in regional and global observed temperature changes: A new dataset from 1850, *J. Geophys. Res.*, *111*, D12106, doi:10.1029/2005JD006548.

Dickson, R. R., J. Meincke, S. A. Malmber, and A. J. Lee (1988), The "great salinity anomaly" in the northern North Atlantic 1968–1982, *Prog. Oceanogr.*, *20*, 103–151.

Enfield, D. B., A. M. Mestas-Nunez, and P. J. Trimble (2001), The Atlantic Multidecadal Oscillation and its relationship to rainfall and river flows in the continental U.S, *Geophys. Res. Lett.*, *28*, 2077–2080.

Frankcombe, L. M., A. von der Heydt, and H. A. Dijkstra (2010), North Atlantic Multidecadal Climate Variability: An investigation of dominant time scales and processes, *J. Clim.*, *23*, 3626.

Hansen, J., R. Ruedy, Mki. Sato, and K. Lo (2010), Global surface temperature change, *Rev. Geophys.*, *48*, RG4004, doi:10.1029/2010RG000345.

Hurrell, J. W. (1995), Decadal trends in the North Atlantic Oscillation and relationships to regional temperature and precipitation, *Science*, *269*, 676–679.

Jones, P. D., and A. Moberg (2003), Hemispheric and large-scale surface air temperature variations: An extensive revision and an update to 2001, *J. Clim.*, *16*, 206–23.

Jones, P. D., T. Jónsson, and D. Wheeler (1997), Extension to the North Atlantic Oscillation using early instrumental pressure observations from Gibraltar and South-West Iceland, *Int. J. Climatol.*, *17*, 1433–1450.

Jungclaus, J. H., H. Haak, M. Latif, and U. Mikolajewicz (2005), Arctic–North Atlantic interactions and multidecadal variability of the meridional overturning circulation, *J. Clim.*, *18*, 4013–4030.

Kerr, R. A. (2000), A North Atlantic climate pacemaker for the centuries, *Science*, 16 *288*(5473), 1984–1985, doi:10.1126/science.288.5473.1984.

Menne, M. J., and C. N. Williams (2005), Detection of undocumented change points using multiple test statistics and reference series, *J. Clim.*, *18*, 4271–4286.

Muller, R. A., and G. MacDonald (2000), *Ice Ages and Astronomical Causes: Data, Spectral Analysis, and Models*, 337 pp., Springer/Praxis, New York.

Munnich, M., M. Latif, S. Venzke, and E. Maier-Reimer (1998), Decadal Oscillations in a Simple Coupled Model, *J. Clim.*, *11*, 3309–3319.

Rohde, R., R. Muller, R. Jacobsen, S. Perlmutter, A. Rosenfeld, J. Wurtele, J. Curry, C. Wickham, and S. Mosher (2013a), Berkeley earth temperature averaging process, *Geoinfor. Geostat.: An Overview 1*, 2, doi:10.4172/gigs.1000103.

Rohde R., R. Muller, R. Jacobsen, E. Muller, S. Perlmutter, A. Rosenfeld, J. Wurtele, D. Groom, and C. Wickham (2013b), A new estimate of the average earth surface land temperature spanning 1753 to 2011, *Geoinfor. Geostat.: An Overview*, *1*, 1, doi:10.4172/gigs.1000101.

Scafetta, N. (2010), Empirical evidence for a celestial origin of the climate oscillations and its implications, *J. Atmos. Sol. Terr. Phys. 72*, 951–970, doi:10.1016/j.jastp.2010.04.015.

Schlesinger, M. E., and N. Ramankutty (1994), An Oscillation in the global climate system of period 65–70 years, *Nature*, *367*, 723–726, doi:10.1038/367723a0.

Sévellec, F., and A. V. Fedorov (2010), Excitation of SST anomalies in the eastern equatorial Pacific by oceanic optimal perturbations, *J. Mar. Res.*, *68*, 597–624.

Sévellec, F., T. Huck, M. Ben Jelloul, and J. Vialard (2009), Non-normal multidecadal response of the thermohaline circulation induced by optimal surface salinity perturbations, *J. Phys. Oceanogr.*, *39*, 852–872.

Thompson, D. W. J., and J. M. Wallace (1998), The Arctic Oscillation signature in the wintertime geopotential height and temperature fields, *Geophys. Res. Lett.*, *25*(9), 1297–1300.

Trenberth, K. E., J. M. Caron, D. P. Stepaniak, and S. Worley (2002), Evolution of El Niño–Southern Oscillation and global atmospheric surface temperatures, *J. Geophys. Res.*, *107*(D8), 4065, doi:10.1029/2000JD000298, 2002.

Zhang, R., and T. L. Delworth (2007), Impact of the Atlantic Multidecadal Oscillation on North Pacific climate variability, *Geophys. Res. Lett.*, *34*, L23708, doi:10.1029/2007GL031601.

Zhang, R., T. L. Delworth, and I. Held (2007), Can the Atlantic Ocean drive the observed multidecadal variability in Northern Hemisphere mean temperature?, *Geophys. Res. Lett.*, *34*, L02709, doi:10.1029/2006GL028683.